

Diagrammatic Analysis of QCD Gauge Transformations and Gauge Cancellations

Y.J. Feng* and C. S. Lam†

*Department of Physics, McGill University,
3600 University St., Montreal, P.Q., Canada H3A 2T8*

Abstract

Diagrammatic techniques are invented to implement QCD gauge transformations. These techniques can be used to discover how gauge-dependent terms are cancelled among diagrams to yield gauge-invariant results in the sum. In this way a multiloop pinching technique can be developed to change ordinary vertices into background-gauge vertices. The techniques can also be used to design new gauges to simplify calculations by reducing the number of gauge-dependent terms present in the intermediate steps. Two examples are discussed to illustrate this aspect of the applications.

1 Introduction

A typical computation in the Standard Model generates many gauge-dependent terms that get cancelled at the end. The labour of calculation can be thus considerably reduced if suitable gauges are chosen to minimize the presence of these terms. As far as propagators goes it is usually simplest to use the Feynman gauge. As to vertices and external gluon wave functions, more unconventional gauges can often lead to greater simplifications.

The spinor helicity technique [1] is a case in point. External gluon wave functions are chosen in lightcone gauges defined by lightlike reference momenta k , which may be different for different gluons. A judicious choice of k 's can reduce the number of terms present, and sometimes even renders whole diagrams zero. This technique was originally designed [2, 3] for tree-level calculations but with superstring [4] and first-quantized [5] techniques it can be extended at least to one-loop diagrams, and with Schwinger representation it can be extended to multiloops [6].

Further simplifications might be obtained by choosing gauges that affect the vertices. The best known example of this kind is probably the background gauge (BG) [7], in which a

triple-gluon (3g) vertex attached to an external gluon contains four terms, two less than the six terms present in a normal 3g vertex. This gauge is particularly convenient for one-loop n -gluon 1PI amplitudes, where each 3g vertex present is such a BG 3g vertex. In addition to this reduction in number, of the four terms in such a vertex, only one involves the internal line and needs to be integrated over. For other diagrams a different gauge may be more convenient. For example, in some sense the Gevais-Neveu gauge [8] is the simplest one for n -gluon diagrams in the tree approximation. It is quite remarkable that in tree and one-loop order, the superstring formalism automatically chooses in some sense these best gauges to compute [4].

From these examples it is clear that the most suitable gauge to use depends on the process and the details of the Feynman diagrams. In order to devise new gauges suitable for a new set of Feynman diagrams, a systematic study of the mechanism for the cancellation of gauge-dependent terms is needed. Since Feynman diagrams are much simpler and more intuitive to visualize than the corresponding analytic expressions, it would be best for the same reason if such gauge cancellations can be cast in diagrammatic languages. This is what we intend to develop in the first part of this article.

How this task is accomplished is well known in QED but not in QCD. In QCD, a one-loop *pinching technique* [9, 10] is known to simplify calculations by converting ordinary vertices to BG vertices, though to our knowledge a general systematic study for multiloop is not available. There are two reasons why cancellation of gauge-dependent terms and gauge transformations are considerably more complicated in QCD than in QED. The first is the complication of color. Fortunately this can be sidestepped by a color decomposition and the use of color-oriented diagrams, as will be discussed in §IIA. The second complication is more substantial, and it relates to the problem of source diffusion. Unlike QED where the charge always resides on the electron lines, the presence of triple and four-gluon vertices spread the color globally throughout the Feynman diagram. In other words, it is the covariant divergence of the color current that is now zero, and not the usual divergence. This global nature means that the local cancellation of gauge-dependence in QED is no longer sufficient for QCD. This additional complication of source diffusion fortunately can be handled by introducing ‘propagating diagrams’, as will be discussed in §IIB.

One may also view the discussion below in another light. Imagine starting out from a classical Yang-Mills theory or a tree-order scattering amplitude. Ghost vertices are absent there. Suppose now loop diagrams are built up via generalized unitarity by gluing together tree diagrams. Ghost loops would still be absent after the gluing so why then do we need them? The reason must be that without them the loop amplitudes will no longer be gauge invariant, but how do we see that? Part of what is being discussed below (Figs. 13–16) can be thought of as a way of seeing that. Alternatively one may think of what is being done below as just another way of deriving the BRST transformation, but this time microscopically, done vertex by vertex and diagram by diagram.

The basic technique for separating the color and for the creating of the ‘propagating diagrams’ will be discussed in the next section, throughout which the gluon propagator is taken to be in the Feynman gauge. This technique is then used to prove *diagrammatically*

known field-theoretic results. In particular covariant-gauges will be taken up in §III, and *multiloop* pinching technique will be discussed in §IV, where we shall show how to create background gauge vertices from ordinary vertices by the *incomplete cancellation* of divergent parts. In §V, we shall discuss two examples for using these techniques to design new gauges. These are just examples and there is no claim that the new gauges are the simplest possible. Nevertheless, it does illustrate that *simpler* gauges can be designed, and hopefully by working harder one can one day design the ‘simplest’ gauge to be used for a given set of diagrams. This latter problem is being studied.

2 Diagrammatic Analysis in the Feynman Gauge

2.1 Color-oriented vertices

If a QCD Feynman amplitude \mathcal{T} is given a color decomposition into a set of independent color tensors \mathcal{C}_i , $\mathcal{T} = \sum_i \mathcal{C}_i a_i$, then each of the color-independent subamplitudes a_i is known to be gauge invariant [1], though how this is achieved diagrammatically, so that individual gauge-dependent diagrams add up to give gauge-independent results, is much less known. In order to study this we must first learn how to compute the subamplitudes a_i diagrammatically.

The relevant diagrams to compute a_i from are the *color-oriented diagrams*. They differ from the ordinary Feynman diagrams in having fixed *cyclic ordering* of the gluon and the ghost lines at all the vertices. Vertices with such ordering imposed are the *color-oriented vertices*; Feynman diagrams made up of color-oriented vertices are the color-oriented diagrams[6]. A single Feynman diagram gives rise to many color-oriented diagrams, differing from one another in the cyclic ordering of the gluon and ghost lines at the vertices. Color-oriented vertices arise from ordinary triple-gluon and ghost vertices by a decomposition of their color factor, $f^{abc} = -i[\text{Tr}(T^a T^b T^c) - \text{Tr}(T^a T^c T^b)]$. This produces two trace terms with fixed cyclic ordering of the fundamental color generators T^a , corresponding to the two color-oriented vertices. Similarly, the decomposition of the color factor $f^{abcd} = (-i)^2[\text{Tr}(T^a T^b T^c T^d) - \text{Tr}(T^b T^a T^c T^d) - \text{Tr}(T^a T^b T^d T^c) + \text{Tr}(T^b T^a T^d T^c)]$ generates color-oriented vertices for an ordinary four-gluon vertex. The color factor at a fermion vertex is given by T^a . It cannot be further decomposed so there is only one color-oriented vertex per ordinary fermion vertex. In that case it does not matter where the gluon line is drawn wrt the quark line.

In an $U(N)$ theory, each color-oriented diagram gives rise to only one color tensor \mathcal{C}_i , determined entirely by the cyclic ordering of the external lines. Thus each a_i is given by the sum of color-oriented diagrams with a fixed external-line ordering. For $SU(N)$ theories, a color-oriented diagram may contain more than one color tensor \mathcal{C}_i , but in what follows we shall only consider those a_i given by the sum of all color-oriented diagrams with a fixed ordering of the external lines.

With color thus factored out, vertex and propagator factors depend on spin and momentum but no longer color. The propagators are the usual ones, being $-1/(\gamma \cdot p - m)$, $-1/p^2$, and $g^{\alpha\beta}/p^2$ respectively for fermions, ghosts, and gluons. Up to a sign the color-oriented

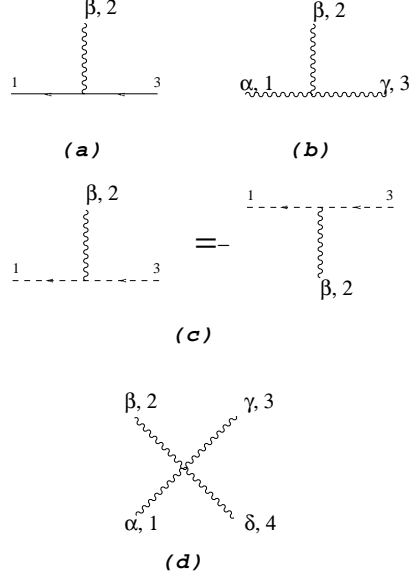


Figure 1: Color-oriented vertices for QCD.

vertices coincide with the ordinary vertices without their color factors. The color-oriented vertices are displayed in Fig. 1; their analytical expressions are given below.

$$F_\beta = g \gamma_\beta , \quad (2.1)$$

$$T_{\alpha\beta\gamma}(p_1, p_2, p_3) = g [g_{\alpha\beta}(p_1 - p_2)_\gamma + g_{\beta\gamma}(p_2 - p_3)_\alpha + g_{\gamma\alpha}(p_3 - p_1)_\beta] , \quad (2.2)$$

$$G_\beta(p_1) = g (p_1)_\beta , \quad (2.3)$$

$$Q_{\alpha\beta\gamma\delta} = g^2 [2g_{\alpha\gamma}g_{\beta\delta} - g_{\alpha\beta}g_{\gamma\delta} - g_{\alpha\delta}g_{\beta\gamma}] . \quad (2.4)$$

All momenta in these formulas are outgoing, except those along the quark lines where they follow the directions of the fermionic arrows. The lines in Fig. 1c may have two possible ordering, as shown. We shall occasionally refer to the one with a positive sign, as given by eq. (1c), to have the *right orientation*, and the one with a minus sign to be of the *wrong orientation*.

2.2 Divergence relations

A gauge transformation changes the longitudinal polarization of a gluon. The corresponding change to a subamplitude is obtained by computing the divergence of a color-oriented diagram, which in turn is obtained by computing the divergence of the color-oriented vertices. These divergences are obtained from eqs. (2.1) to (2.4) to be

$$(p_2)^\beta F_\beta = g [-(\gamma \cdot p_1 - m) + (\gamma \cdot p_3 - m)] , \quad (2.5)$$

$$(p_2)^\beta T_{\alpha\beta\gamma}(p_1, p_2, p_3) = g g_{\alpha\gamma} p_1^2 - g g_{\alpha\gamma} p_3^2 - (p_1)_\alpha G_\gamma(p_1) + (p_3)_\gamma G_\alpha(p_3) , \quad (2.6)$$

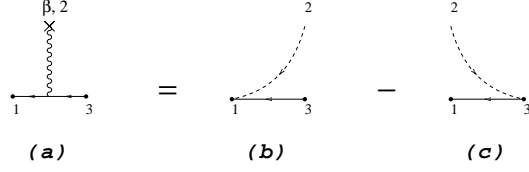


Figure 2: Divergence relation for the gluon-quark vertex.

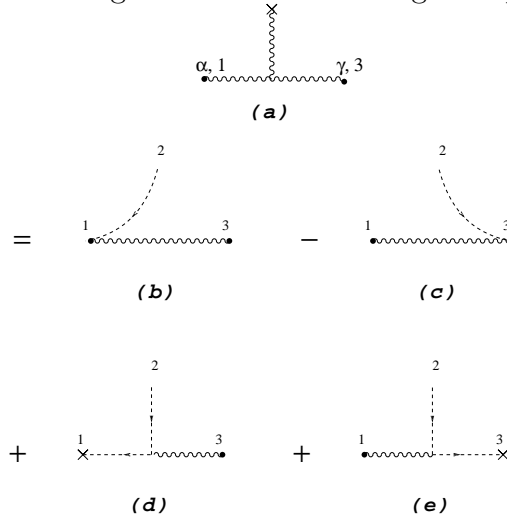


Figure 3: Divergence relation for the triple gluon vertex.

and

$$(p_2)^\beta G_\beta(p_1) + (p_3)^\gamma G_\gamma(p_1) + g p_1^2 = 0 , \quad (2.7)$$

$$(p_2)^\beta Q_{\alpha\beta\gamma\delta} - g T_{\alpha\gamma\delta}(p_1 + p_2, p_3, p_4) + g T_{\alpha\gamma\delta}(p_1, p_2 + p_3, p_4) = 0 . \quad (2.8)$$

The resulting terms have been arranged to be proportional either to a propagator or a vertex so that these relations can be expressed diagrammatically, as in Figs. 2 to 5. A cross in a gluon line represents the divergence, *i.e.*, a factor p_α for the gluon with outgoing momentum p and Lorentz index α . A cross at the end of a (dotted) ghost line is meant to be a cross on the gluon line it is connected to. Namely, if p is the outgoing momentum of the ghost line so that $-p$ is the outgoing momentum and α the Lorentz index of the gluon line it is connected to, then a cross at the end of the ghost line indicates a factor $-p_\alpha$. The propagators in Figs. 2b, 2c, 3b, 3c, 4c, 5b, and 5c have been cancelled out to obtain these *sliding diagrams*, so called because they can be obtained by converting the original gluon line into a sliding external ghost (dotted) line. Diagrams 3d and 3e serve to propagate the cross along the original gluon lines and will thus be called the *propagating diagrams*. A propagating cross always drags a ghost line behind it replacing the original gluon line.

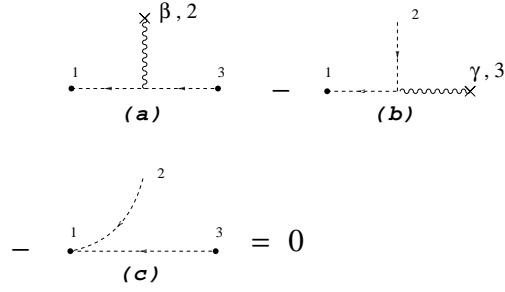


Figure 4: Divergence relation for the ghost vertex.

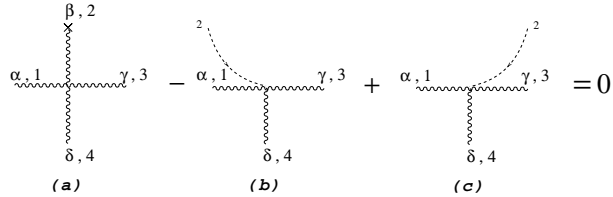


Figure 5: Divergence relation for the four-gluon vertex.

QED requires only Fig. 2. What makes QCD complicated is the presence of many more vertices and divergence relations, and the existence of these propagating diagrams relating to the source diffusion problem discussed in the Introduction.

Possibly with the exception of Fig. 4, these divergence relations have a regular structure which we shall call the *canonical structure*. On the rhs of these divergence relations there are always two sliding diagrams with opposite signs, arranged so that the signs obtained from a triple-gluon vertex are opposite to the signs obtained from a four-gluon vertex. There are no propagating diagrams for the four-gluon vertex, but both of the propagating diagrams emerging from the triple-gluon divergence relation carry a + sign. It turns out that it is this regular canonical structure that guarantees the gauge invariance of the sum of diagrams.

In the sliding diagrams, the external ghost line serves to inject a coupling-constant factor g as well as the momentum of the original gluon (p_2) into the line it is tangential to, but otherwise it is inert. Thus if the ghost slides into a momentum-independent vertex, or is tangential to a line whose momentum the vertex does not depend on, then the new vertex with the extra ghost line is equal to the old vertex without it, as shown in Figs. 6, 7, and 8. However, triple-gluon vertices are momentum-dependent so Figs. 5b and 5c are not identical, though their difference is simply given by 5a.

The signs appearing in Figs. 3d and 3e require an explanation. First, the crosses in these diagrams are respectively $-(p_1)_\alpha$ and $-(p_3)_\gamma$. Secondly, the original gluon *propagators* for line 1 in Fig. 3d, and line 3 in 3e, are now replaced by ghost *propagators*, resulting in an extra minus sign for both. Thirdly, an extra minus sign is attached to the ghost vertex in Fig. 3d because of its wrong orientation. Putting these three things together, the signs in front of 3d and 3e are both +, a fact which becomes very important later on for ghost cancellation.

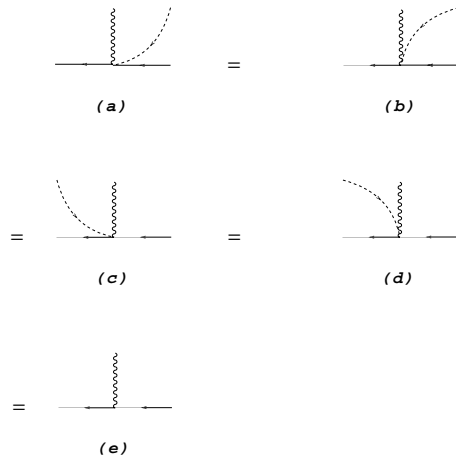


Figure 6: Relations between sliding diagrams.

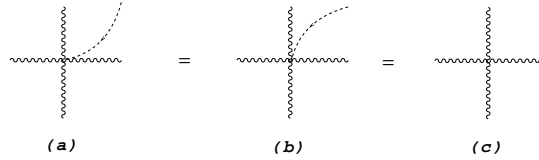


Figure 7: Diagrams with a ghost line sliding into a four gluon vertex.

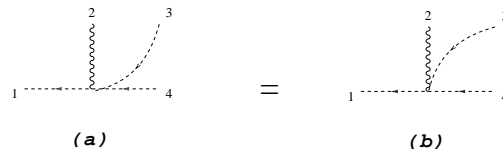


Figure 8: Ghost vertex with an extra ghost sliding in.

Eqs. (2.5) and (2.6) (Figs. 2 and 3) can be used repeatedly to compute the divergence of a color-oriented diagram. This iteration terminates when the cross either rests on (i) an external line, (ii) a four-gluon vertex like Fig. 5a, or (iii) a ghost vertex like Fig. 4a, or that (iv) there is no longer any cross in the diagram. If (iv) happens, it is possible for the sliding ghost line to end up (iv a) at another external line, (iv b) at a fermion vertex like Fig. 6, (iv c) at a four-gluon vertex like Fig. 7, (iv d) at a ghost vertex like Fig. 8, or (iv e) at a three-gluon vertex like Fig. 5b or 5c.

2.3 Notations and conventions

By a ‘diagram’ we always mean a color-oriented diagram from now on. By the ‘sum of all diagrams’ we always mean the sum of all color-oriented diagrams with the same ordering of the external lines as the original diagram.

There are more diagrams in this paper than equations. In order not to confuse diagram numbers with equation numbers, we will adhere to the convention that a number not prefixed by Fig. or eq. is taken to mean a *diagram number*.

A diagram is said to be *on-shell* if all its external lines are on-shell. It is said to be *on-shell/crossed* if all its external lines are either on-shell, or are off-shell gluon lines carrying a cross. Most of the following results apply either to on-shell diagrams, or on-shell/crossed diagrams.

2.4 Gauge transformation of color-oriented diagrams

We consider now how a color-oriented diagram changes when the wave function of an external gluon line undergoes a gauge variation. The *change* is proportional to the divergence, represented graphically by a cross at the end of the external gluon line. This produces many diagrams by using 2 and 3, each satisfying one of (i) to (iv) at the end of §IIB.

We shall now show that the *net change* from the sum of all diagrams vanishes if the diagrams are on-shell. This occurs because each resulting diagram either vanishes by itself, or they combine to cancel each other in pairs or in threesome. In the process of the proof we will also discover what remains if some of the external lines are taken off-shell. These will turn out to be precisely those diagrams required by the BRST transformations.

These conclusions are certainly of no surprise. What we gain by carrying out these analyses is the knowledge how this is realized diagrammatically.

It is simplest to consider first diagrams satisfying condition (iv). When (iv a) is satisfied, the external ghost ends on another external line. The pair of ghost/external lines no longer possesses a particle pole to overcome the Klein-Gordon zero in front of the LSZ reduction formula, so such diagrams do not contribute to on-shell scattering amplitudes. If the external line is off-shell this diagram survives, as is demanded by the BRST transformation.

Next, suppose (iv b) happens. Then using Fig. 6 a pairwise cancellation takes place as shown in Fig. 9, where diagrams 9a and 9b to the left of the arrow are the diagrams from which 9c and 9d come from one step back in the transformation. Note that Fig. 9,

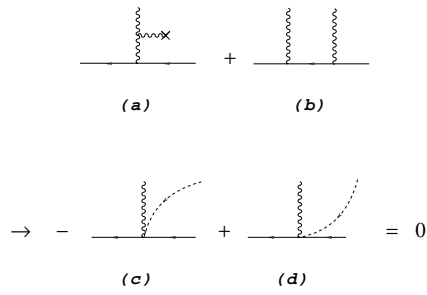


Figure 9: Local gauge cancellation near a quark vertex.

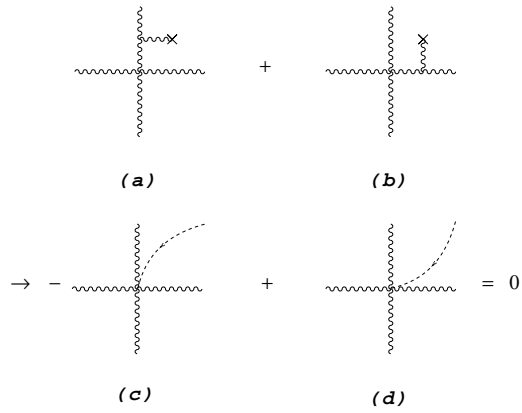


Figure 10: Local gauge cancellation near a four-gluon vertex.

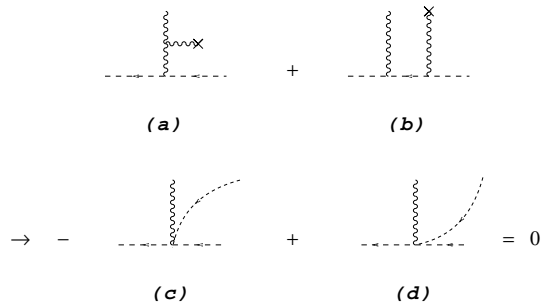


Figure 11: Local gauge cancellation near a ghost vertex.

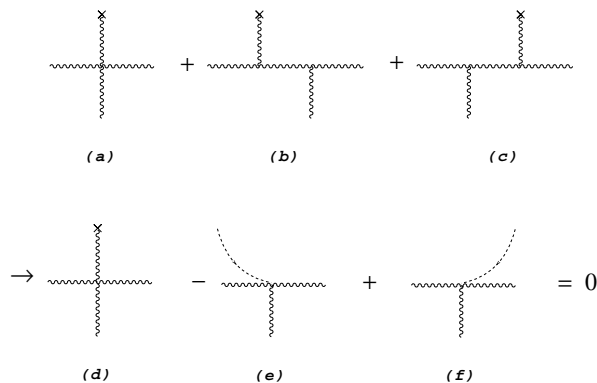


Figure 12: Local gauge cancellation near a three-gluon vertex.

and similarly for all the diagrams considered below, is meant to be a part of a much larger color-oriented diagram, and not necessarily a whole diagram by itself.

Similar pairwise cancellation occurs for (iv c) and (iv d) as shown in 10 and 11. Using 5, case (iv e) combines with case (ii) to give a threesome cancellation as shown in Fig. 12.

Strictly speaking, there is one more case under (iv d) which we have not yet considered, namely, when the external ghost line slides into a quadrant bounded by the *outgoing* ghost line, as shown in 15a and 15b. This case will be considered at the end. There are two reasons for the asymmetry between this case and 11, both arising from the asymmetry of the ghost vertex, which depends on the momentum of the outgoing ghost but not the incoming ghost, nor the gluon. As a result, the sliding term in 4 slides only to the left but not to the right. Moreover, Fig. 8 is true, but there is no corresponding relation when the external sliding ghost lies between the gluon and the *outgoing* ghost.

We must now deal with cases where the external ghost line ends at a cross. Case (ii) has already been dealt with but we still have to consider cases (i) and (iii). Case (i) is simple. If that external line the cross ends on is on-shell, then the amplitude vanishes because external gluon wave functions are divergenceless. Otherwise this diagram remains as required by the BRST transformations.

The identity in Fig. 4 is required to deal with case (iii). It is important in this connection to note that the ghost line appearing in 4a must be an internal ghost line, forming a closed loop as in 13a. This means that the identity in 4 will always look like the identity in 13, so the only question left is where 13b and 13c will come from. With the presence of the ghost loop in 13a, there must be a diagram where the ghost loop is replaced by a gluon loop, as in 14a. Using 3d, 3e repeatedly on 14a, we shall end up with a diagram that looks like 13b=14b. The minus sign in front of 13a comes from the ghost loop factor and there is no corresponding minus sign for the gluon loop in 14a. In addition to 13a, there is a diagram like it but the gluon with the cross is linked up directly with the other gluon, as in 14c. The $-$ sign in front is again due to the ghost loop. Using 3c and then the equality in Fig. 8, 14c produces 14d=13c. The three diagrams in Fig. 13 cancel one another by using Fig. 4. The

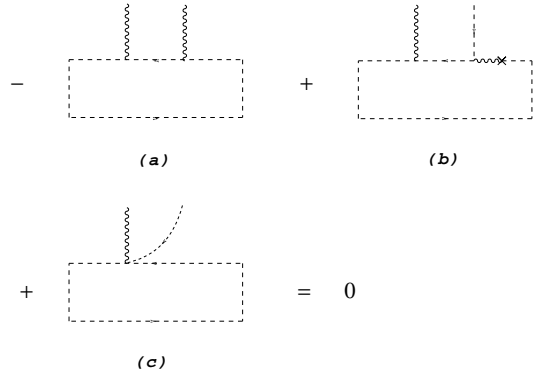


Figure 13: Cancellation involving ghost loop. Same as Fig. 4 with ghost loop explicitly drawn in.

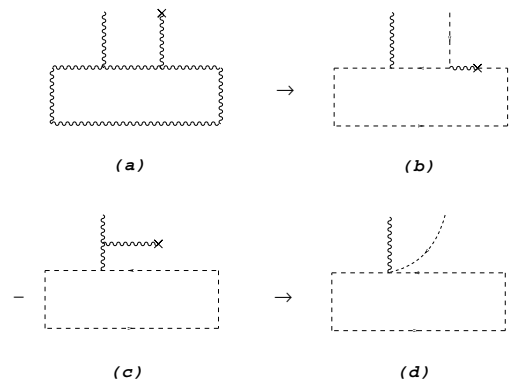


Figure 14: How 13b and 13c are produced from color-oriented diagrams.

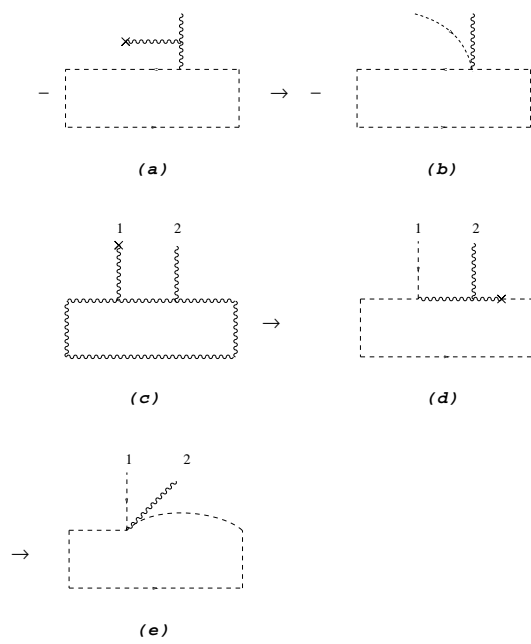


Figure 15: How 16a and 16b are produced from color-oriented diagrams.

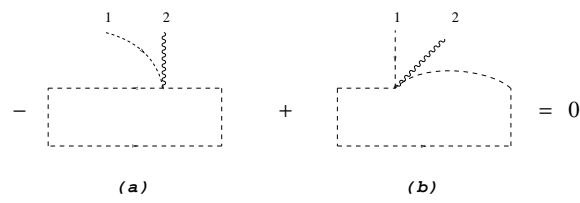


Figure 16: Pairwise cancellation for the other situation of case (iv d).

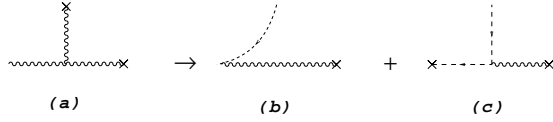


Figure 17: Double-divergence relation of the triple gluon vertex.

same proof will go through if the arrow of the ghost loop in 13a runs clockwise instead.

There is one final case which we have not yet dealt with, namely, the other situation of case (iv d) which we skipped before. Consider 15a, where the explicit $-$ sign in front is again the ghost loop factor. Using 3b, this is transferred to 15b=16a, with the external ghost between the gluon and the *outgoing* internal ghost line. Its cancellation comes from the gluon-loop diagram shown in 15c. Using 3d and 3e, 15c is transformed into 15d, which by 3b, becomes 15e=16b. Now 16a+16b=0 because the vertices in these two diagrams are simply the same vertex drawn a bit differently.

In summary, we have shown that the sum of all on-shell diagrams with a cross at the end of a gluon line is zero.

3 Covariant Gauges

The gluon propagator in a covariant gauge is $(g^{\alpha\beta} + \xi p^\alpha p^\beta / p^2) / p^2$. In the last section divergence relations and gauge invariances of the external gluons were shown in the Feynman gauge $\xi = 0$. The effect of $\xi \neq 0$ will be discussed in the present section, using the same techniques developed in the last.

The only additional tool needed for the following analysis is the double-divergence relation

$$\begin{aligned}
 (p_3)^\gamma (p_2)^\beta T_{\alpha\beta\gamma}(p_1, p_2, p_3) = & \quad g (p_3)_\alpha p_1^2 \\
 - & \quad (p_1)_\alpha (p_3)^\gamma G_\gamma(p_1) ,
 \end{aligned} \tag{3.9}$$

obtainable from eq. (2.6) by taking the divergence wrt p_3 on both sides. Diagrammatically, this can be represented by Fig. 17, which is the same as Fig. 3 with 3b and 3e removed and with an additional cross added to the third gluon line. A convenient way to visualize this is to regard Fig. 3 to be true in all cases, with or without an additional cross on line 3, but to add to that the additional rule that the ghost line on the rhs must avoid coming into contact with any additional crosses. This rule effectively eliminates 3b and 3e as required.

This double-divergence relation allows us to generalize the result of the §IID into

Lemma 1: *The sum of all on-shell/crossed diagrams with a cross on one of the external*

gluon lines is zero, if all gluon propagators are taken in the Feynman gauge.

This lemma is more general than what has been proved because the external lines with a cross on them do not have to be on-shell, so diagrams of types (iv a) and (i) with the external ghost resting on them will no longer vanish. However, such diagrams can never occur because of eq. (3.1), which as noted before may be taken to say that the external ghost line must avoid the additional crosses now situated at the end of the off-shell gluon lines.

This lemma can be used to show the independence of the gauge parameter ξ .

Lemma 2 *The sum of on-shell/crossed diagrams is independent of the gauge choice of every gluon propagator.*

The gauge-dependent part of a gluon propagator is of the form $\xi p^\alpha p^\beta / p^2 / p^2$. Except for the additional factor $\xi / p^2 / p^2$, the ξ -dependent part can be represented diagrammatically by breaking the internal line into a pair of external lines, each with a cross at the end. In this way two diagrams are generated by each gluon propagator: one being the original diagram with the propagator in the Feynman gauge, and the other obtained by breaking this propagator into a pair of external lines with a cross at the end of each.

If a diagram has m propagators, then this procedure breaks it up into 2^m diagrams. When we sum up all possible on-shell/crossed diagrams, the sum becomes 2^m sets of sums, each of which satisfies Lemma 1, so Lemma 2 is proved.

4 Pinching Technique and the Background Gauge

The technique developed in §II can also be used to manipulate the divergence part of a triple-gluon vertex. Such vertex manipulations had previously been used to simplify one-loop calculations, and in that context it is known as the *pinching technique* [8]. To one-loop order it has been shown that pinching technique gives rise to the *background gauge* (BG). In what follows we generalize this approach to *multiloops* to show how to convert the normal vertices into the BG vertices.

4.1 BG vertices

The BG color-oriented vertices consist of the original vertices in Fig. 1 (eqs. (2.1) to (2.4)), plus the additional vertices in Fig. 18 given by the following formulas:

$$18a = g [g_{\gamma\alpha}(p_3 - p_1)_\beta - 2g_{\alpha\beta}(p_2)_\gamma + 2g_{\beta\gamma}(p_2)_\alpha] , \quad (4.10)$$

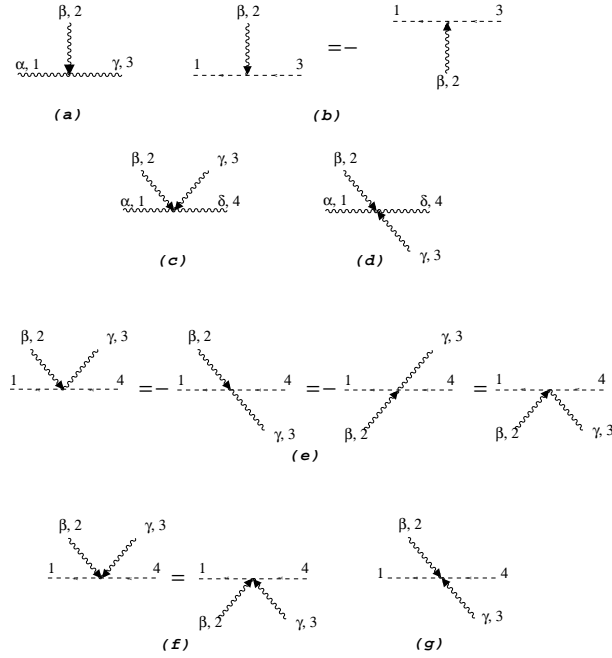


Figure 18: Color-oriented BG vertices with at least one arrowed (external) line.

$$18b = g (p_1 - p_3)_\beta , \quad (4.11)$$

$$18c = g [-g_{\beta\gamma}g_{\alpha\delta} - 2g_{\alpha\beta}g_{\gamma\delta} + 2g_{\alpha\gamma}g_{\beta\delta}], \quad (4.12)$$

$$18d = -2g g_{\beta\gamma}g_{\alpha\delta} , \quad (4.13)$$

$$18e = g g_{\beta\gamma} , \quad (4.14)$$

$$18f = g g_{\beta\gamma} , \quad (4.15)$$

$$18g = -2g g_{\beta\gamma} . \quad (4.16)$$

Gluon lines with an arrow are to be distinguished from gluon lines without an arrow. In this section we follow the traditional usage to assume all arrowed lines to be external gluon lines, though the reverse is not true. Vertices attached to external gluon lines should be taken from 18 whenever possible, but if they are absent from 18, then they should be taken from 1. For example, triple-gluon vertices with two external gluons and quark-gluon vertices with an external gluon are not to be found in 18, so they should be taken from 1b and 1a respectively.

It is this distinction between external and internal gluons that produces so many vertices in the BG. In spite of this complication, it is often still simpler to calculate loop processes with a large number of external gluon lines in the BG, because of its reduced dependence on the internal momenta of a triple-gluon vertex. BG is also the gauge that emerges naturally in superstring calculations for 1PI diagrams [3].

The equivalence between the ordinary and the BG vertices is stated in the following

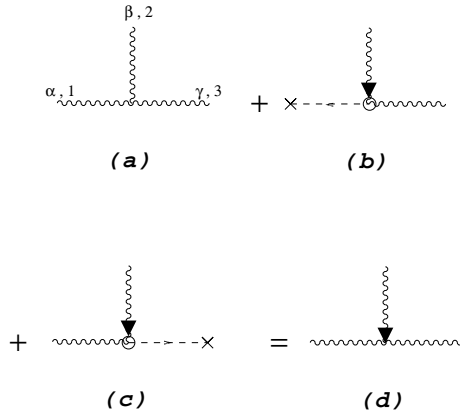


Figure 19: Relation between the triple-gluon vertices 1b and 18a.

lemma.

4.2 Lemma 3

The sum of on-shell/crossed diagrams are not affected when the vertices attached to any number (n) of external gluon lines are changed from the ordinary vertices (Fig. 1) to the BG vertices (Figs. 1 and 18).

4.3 Creation of the new BG vertices

To prove Lemma 3 we need to know how the new BG vertices in Fig. 18 are related to the ordinary vertices in Fig. 1. These relations can be obtained from a relation between 1b and 18a, or equivalently between eqs. (2.2) and (4.1), shown graphically in Fig. 19. For this purpose it is necessary to introduce a new vertex with two gluon and one ghost lines (19b and 19c), joined together by a circle representing the factor $\pm g g_{\mu\nu}$, where μ, ν are the Lorentz indices of the two gluon lines. The sign is taken to be $+$ for 19c and $-$ for 19b. This sign convention is chosen to be the same as the ordinary ghost vertex 1c if the incoming ghost line is replaced by the arrowed gluon line. In the terminology introduced below eq. (2.4), 19c has the right orientation and 19b has the wrong orientation. From now on we shall refer to the vertices 19b,c as the *funny vertices*.

Fig. 19 is used to convert an ordinary vertex 19a to a BG vertex 19d. The two extra terms 19b and 19c will be shown to be instrumental in converting other ordinary vertices into BG vertices. The proof proceeds by induction on n , the number of external lines at which such conversion of vertices is desired.

Suppose $n = 1$ and an ordinary vertex 19a attached a single external gluon line is converted into the BG vertex 19d. The effect of the extra term 19b will now be explained, and an analogous result exists for 19c. If we remove the bulk of the vertex 19b from a

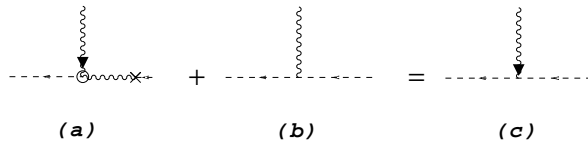


Figure 20: Generation of the ghost vertex 18b.

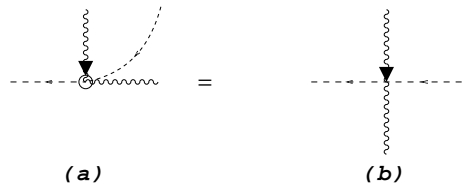


Figure 21: Generating the ghost vertex 18e.

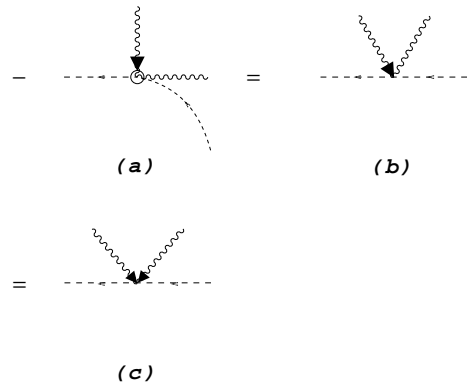


Figure 22: Generating the ghost vertices 18e and 18f.

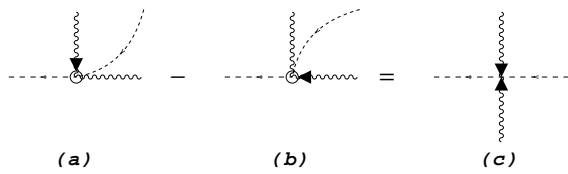


Figure 23: Generating the ghost vertex 18g.

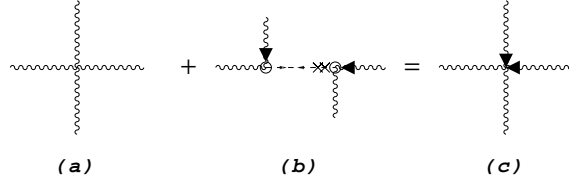


Figure 24: Generating the four-gluon vertex 18c.

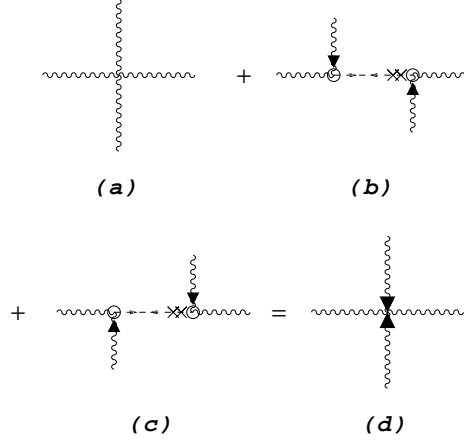


Figure 25: Generating the four-gluon vertex 18d.

diagram except for its cross, Lemma 1 is applicable to the remaining diagram, so the extra diagrams generated by 19b will add up to zero, except when the crosses in 19b is returned by propagation to the same vertex via a gluon loop. In that case 19b gives rise to 20a, in which the gluon loop linking the two sides of the funny vertex is now converted to a ghost loop trailing the cross. There exists another diagram where the gluon loop is replaced by the ghost loop, in which the ordinary ghost vertex 20b appears. The combination of 20a and 20b now gives rise to the BG ghost vertex 20c. An extra minus sign from the ghost loop has been incorporated in front of 20a to make the combined sign + as shown. However, analytically 20a contributes a minus sign because of the wrong orientation of the funny vertex.

The only other way the cross in 19b can return is through a sliding diagram 3b at the last step, thus producing 21a or 22a. Since the propagating cross always drags a ghost line behind it, the gluon loop through which the cross returns has now been changed into a ghost loop and an examination of eqs. (4.5) and (4.6) shows that 21a is the same as 21b=18e and 22a is the same as 22b=18e and 22c=18f.

We have therefore completed showing Lemma 3 when $n = 1$, because none of the other BG vertices in 18 are present for $n = 1$.

We will now proceed to $n = 2$ and assume the first vertex to have been converted already into BG vertices. We must now examine the effect of converting the second vertex from ordinary to BG vertices, again using the relations in 19. Clearly as in the case $n = 1$, there is no problem is converting the second vertex into BG vertices if it were alone. But with

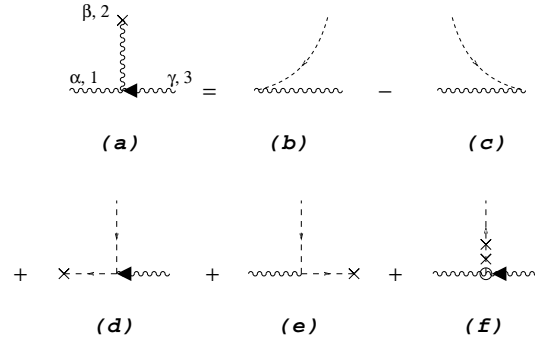


Figure 26: Divergence relation of the BG triple-gluon vertex 18a.

$n = 2$, there is now the possibility of an interaction between the two vertices to cause a change.

To start with, we can no longer use Fig. 3 to propagate the cross beyond the first vertex because the triple-gluon vertex here is already a BG vertex. We must therefore work out a relation analogous to 3 but valid for the BG triple-gluon vertex. This is obtained from eq. (4.1) and shown in 26, with 26f being $-g g_{\alpha\gamma}(p_2)^2$. It is important to note that this divergence still possesses a regular structure. As before, we have the sliding diagrams with opposite signs (26b and 26c), the propagating diagrams with plus signs (26d and 26e), but there is now a new *stagnant diagram* involving the funny vertex (26f) with a single ghost line that goes nowhere. The analytical expression for this term is $-p_2^2 g_{\alpha\gamma}$, with a minus sign on account of the wrong orientation of the funny vertex. Note also that the gluon line in 26d has an arrow but not the one in 26e, ‘because’ that is how it is inherited from 26a.

Although this is getting ahead of ourselves, it would be useful for the sake of comparison to examine this *modified canonical structure* for other divergence relations obtained from eqs. (4.1) to (4.7), and shown in Figs. 27 to 32. There are unfortunately many divergence relations, but this cannot be helped because there are many BG vertices, and because there are many external-line/cross combinations in taking the divergence of 1d. Nevertheless, all these relations possess the sliding diagrams with the canonical signs, the propagating diagrams with plus signs, and the stagnant diagrams with minus signs. External lines are inherited, vertices that do not make sense will not appear, and in the case of the divergence of a four-gluon vertex, the cross is not allowed to propagate through an arrowed line. This last rule is ‘why’ there are no propagating ghosts from the top to the bottom gluon lines in 27, for example. The reason ‘why’ there is no propagating ghost from the top to the left line in Fig. 29 is because the resulting BG ghost vertex does not exist (the arrowed line is not adjacent to the outgoing ghost).

The signs contained in this modified canonical structure are precisely correct to make the extraneous diagrams cancel, extraneous meaning those not needed to produce new BG vertices. For example, consider the combination of diagrams 33a, 33b, and 33c. By using 3 and then 26, 33b produces 33e and 33f, and 33c produces 33g. Using 29, these combine to cancel, leaving behind only the propagating diagram 33h to move on to other vertices.

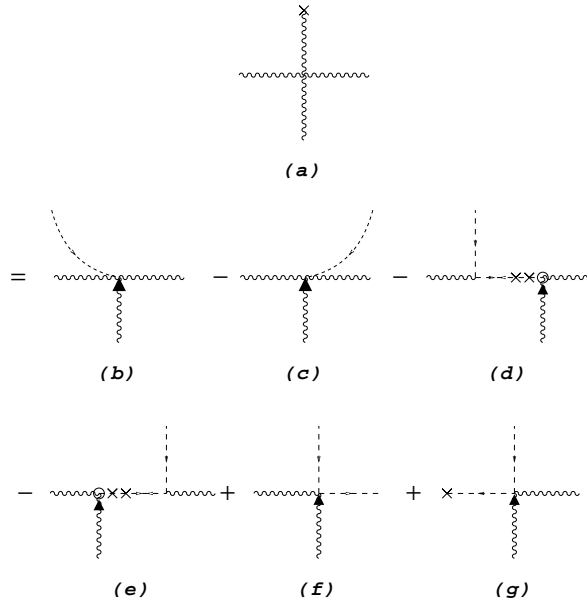


Figure 27: Divergence relation of the four-gluon vertex 1d expressed in terms of BG vertices. The cross is opposite to the external line in the four-gluon vertex.

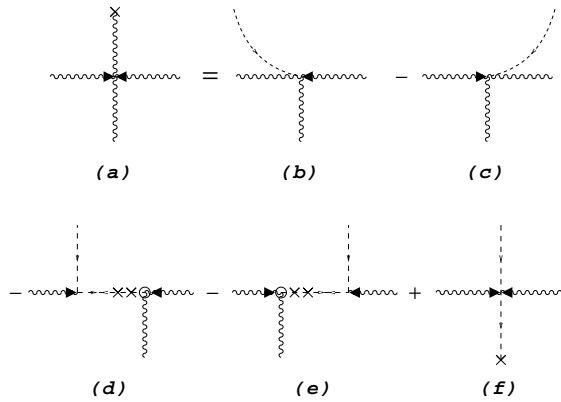


Figure 28: Divergence relation of the four-gluon vertex 18d expressed in terms of the BG vertices.

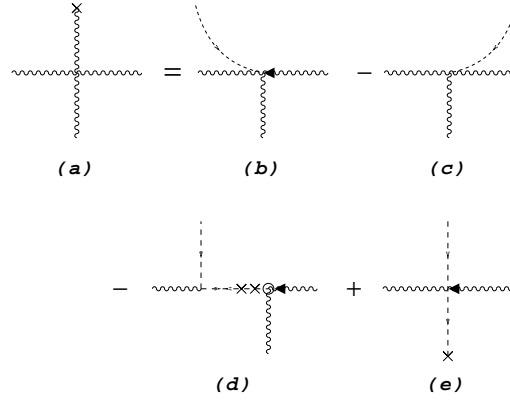


Figure 29: Divergence relation of the four-gluon vertex 1d expressed in terms of BG vertices. The cross is adjacent to the external line in the four-gluon vertex.

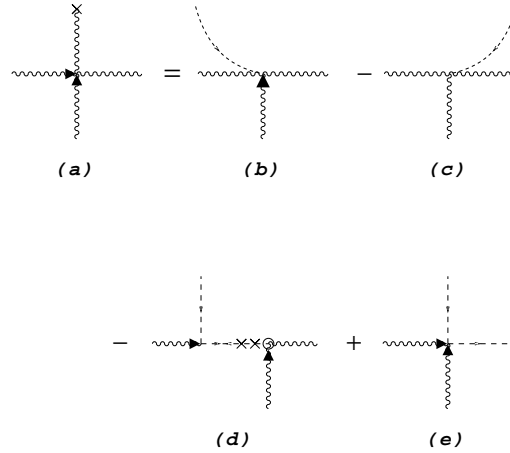


Figure 30: Divergence relation of the four-gluon vertex 18c expressed in terms of the BG vertices.

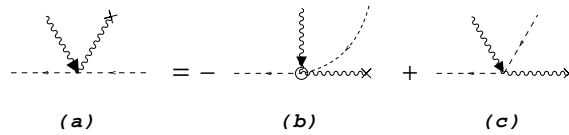


Figure 31: Divergence relation of the ghost vertex 18e expressed in terms of the BG vertices. The cross is adjacent to the arrowed line.

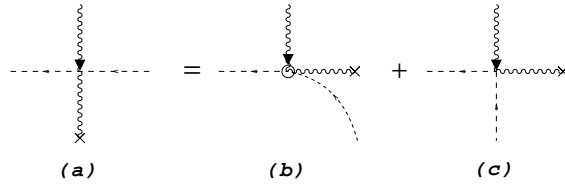


Figure 32: Divergence relation of the ghost vertex 18e expressed in terms of the BG vertices. The cross is opposite to the arrowed line.

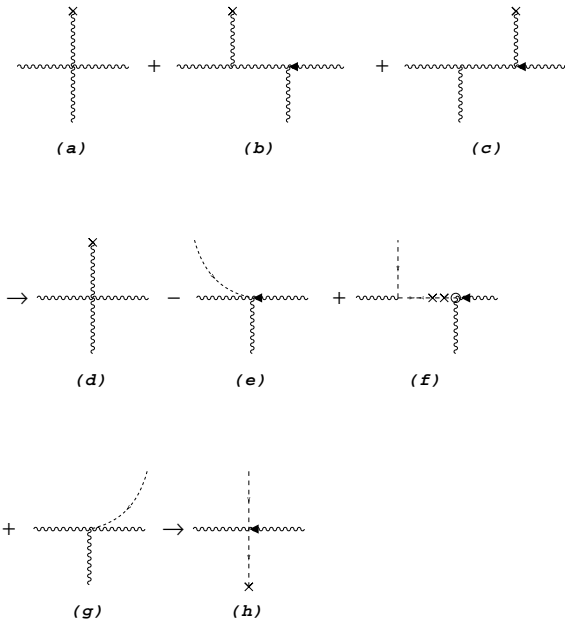


Figure 33: An example of local gauge cancellations, leaving behind just a propagating term to work on another vertex.

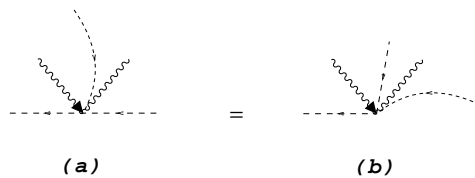


Figure 34: Equality of a ghost line sliding into the ghost vertices 18e.

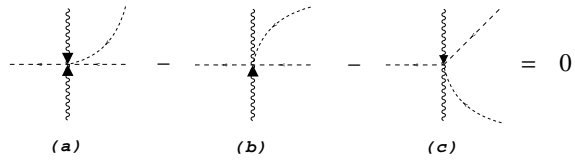


Figure 35: Equality of a ghost line sliding into the ghost vertices.

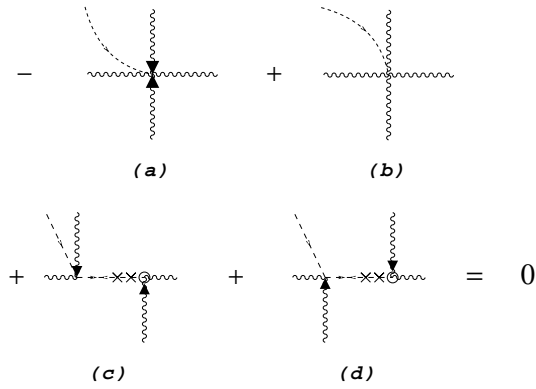


Figure 36: Equality of a ghost line sliding into four-gluon vertices.

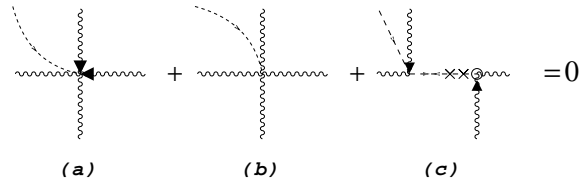


Figure 37: Equality of a ghost line sliding into four-gluon vertices.

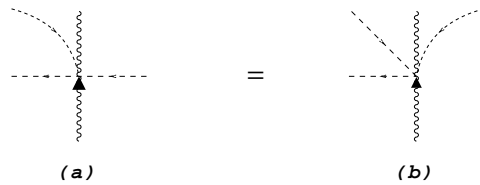


Figure 38: Equality of a ghost line sliding into the ghost vertices 18e.

Similar cancellation takes place in all other cases, if we take into account other identities shown in 34 to 38.

It is important to remark that in the definition of the BG vertices 18 to 25, as well as in the divergence relations 26 to 32, all the external lines may be taken off-shell.

Let us now return to the construction of the BG vertices for $n = 2$, and consider the effect of the cross 19b originating from the second vertex reaches the first (BG) vertex. Because of the modified canonical structure of 26, things proceed similarly to Lemma 1 and 2. Various situations can happen when this cross returns to vertex 2 via a gluon loop. A sliding contribution just before it returns to the second vertex gives rise to 21 to 23.

If the first vertex is just to the right of the second vertex, then in using 19 to convert the second vertex, the contribution of 19c followed by 26 on the first vertex produces terms like 24b, 25b, and 25c. When combined with ordinary four-gluon vertex attached to these two external lines, the BG vertices 24c and 25d are produced.

This completes the proof of Lemma 3 for $n = 2$. For $n > 2$, it is easy to see that nothing new can happen, in the sense that three or more vertices can interact only pairwise. This then completes the proof of the Lemma for all n .

5 Examples of new gauges

The technique developed in §II was used in §III to show the independence of the gauge used in gluon propagators, and in §IV to convert ordinary to BG vertices. There is no reason why it cannot be used to study other gauge problems, including our eventual hope to find the ‘best’ gauge for computing a specific set of gauge-invariant diagrams.

In the present section, we will discuss two unconventional gauges, one for four-gluon tree amplitude and the other for two-loop gluon self-energy diagrams. The new gauges carry fewer terms than either the ordinary or the BG gauge. Though they may not be the ‘best’ gauge possible for the specific problems, nevertheless, it does illustrate the fact that improvements can be made on existing gauges using the techniques developed in this paper.

The tree-diagram example is given in Fig. 39, where the arrowed vertices are given in 18 (eq. (4.1) and (4.4)). It can be shown using the techniques above that a new gauge containing the vertices in these diagrams does exist, *viz.*, the three diagrams in 39 do sum up to give the four-gluon on-shell scattering amplitude.

Note that this is *not* the BG gauge. Since all the four lines in 39a are external, vertex 1d should be used in the background gauge instead of 39a. Moreover, each of the two 3g vertices in 39b,c contains two external lines, again 1b rather than 18a should have been used in the background gauge. In other words, there is no difference between the BG and the ordinary gauge in this process.

Fig. 39a contains one term but the corresponding vertex in BG contains 3 terms. Each of 39b,c contains $4^2 = 16$ terms whereas the corresponding diagrams in BG each contains $6^2 = 36$ terms. Thus the new gauge depicted in 39 saves a total of 42 terms out of the 75 terms needed in the BG.

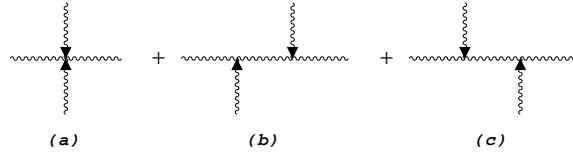


Figure 39: Four-gluon tree amplitude in a new gauge.

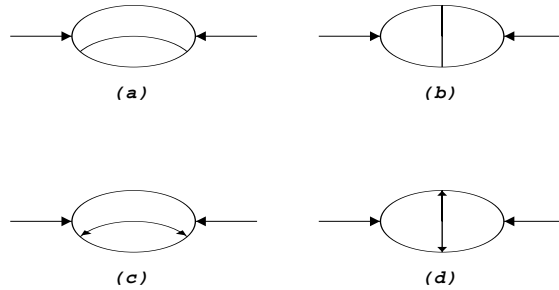


Figure 40: Diagrams with two gluon loops for the gluon self-energy in the BG gauge (a and b) and in the new gauge (c and d).

The two-loop example is given in Fig. 40, where for easy drawing solid lines are used to denote gluons. 40a and 40b are the two-gluon-loop diagrams in BG, whereas 40c and 40d are the same diagrams in the new gauge. Again the arrowed vertices are those displayed in 18. The two-loop gluon self-energy contains a total of 18 diagrams in BG, but owing to incomplete cancellation of the divergence terms when we shift gauges, new vertices and new diagrams are generated and a total of 26 diagrams appeared in this new gauge. Nevertheless, the new gauge still contains few terms in total, because the largest number of terms for each gauge already occurs in the diagrams shown. The BG contains a total of 1242 terms, of which 1152 are contained in 40a,b. In contrast, the new gauge contains a total of only 766 terms, of which 512 are contained in 40c and 40d. In other words, 62% more labour is required to compute the two-loop self energy in BG than in the new gauge, and clearly even more labour is required to compute it in the ordinary gauge.

Other details of this gauge and the two-loop computation will appear separately.

6 Acknowledgments

This research is supported in part by the Natural Science and Engineering Research Council of Canada and by the Québec Department of Education. YJF acknowledges the support of the Carl Reinhardt Major Fellowship. CSL thanks F. Wilczek for discussions and hospitality at the Institute for Advanced Study in Princeton where part of this manuscript was written.

References

- [*] e-mail address: feng@physics.mcgill.ca
- [†] e-mail address: lam@physics.mcgill.ca
- [1] R. Gastmans, Tai Tsun Wu, *The Ubiquitous Photon Helicity method for QED and QCD*, Clarendon Press (1990).
M. L. Mangano, S. J. Parke, Phys. Rep. **200**, 301 (1991).
- [2] F. A. Berends, R. Kleiss, P. De Causmaecker, R. Gastmans, W. Troost and T. T. Wu, Phys. Lett. **103B**, 61 (1982); **239B**, 382, 395 (1984); **264B**, 243, 265 (1986).
- [3] Z. Xu, D. -H. Zhang, and L. Chang, Tsinghua University, Beijing, China, Report No. TUTP-84/4 (unpublished); Report No. TUTP-84/5 (unpublished); Report No. TUTP-84/6 (unpublished); Nucl. Phys. **B298**, 653 (1988).
- [4] Z. Bern and D. C. Dunbar, Nucl. Phys. **B379**, 397 (1992).
Z. Bern and D. A. Kosower, Phys. Rev. Lett **66**, 1669 (1991); Nucl. Phys. **B362**, 389 (1991), **B379**, 451 (1992).
Z. Bern, L. Dixon, and D. A. Kosower, Phys. Rev. Lett. **70**, 2677 (1993).
- [5] M. Strassler, Nucl. Phys. **B385**, 145 (1992); SLAC Report No. SLAC-PUB 5978, 1992 (unpublished).
M. G. Schmidt and C. Schubert, Phys. Lett. **331B**, 69 (1994).
- [6] C. S. Lam, Nucl. Phys. **B397**, 143 (1993) ; Phys. Rev. D **48**, 873 (1993); Can. J. Phys. **72**, 415 (1994).
Y. J. Feng and C. S. Lam, Phys. Rev. D **50**, 7430 (1994).
- [7] B. S. DeWitt, Phys. Rev. **162** (1967) 1195, 1239, in *Dynamic theory of groups and fields* (Gordon and Breach, 1965).
G. 't Hooft, Nucl. Phys. **B62**, 444 (1973).
L. F. Abbott Nucl. Phys. **B185**, 189 (1981).
- [8] L. L. Gervais and A. Neveu, Nucl. Phys. **B334**, 605 (1972).
- [9] J. M. Cornwall, in *Proceeding of the French-American Seminar on Theoretical Aspects of Quantum Chromodynamics*, Marseillee, France, 1981, edited by J. W. Dash (Centre de Physique Théorique, Marseille, 1982).
J. M. Cornwall, Phys. Rev. D **26**, 1453 (1982).
J. M. Cornwall and J. Papavassiliou, Phys. Rev. D **40**, 3474 (1989).
J. Papavassiliou, Phys. Rev. D **41**, 3179 (1990); Phys. Rev. D **46**, 3104 (1993); Phys. Rev. D **47**, 4728 (1993).

- [10] A. Denner, G. Weiglein, and S. Dittmaier, Phys. Lett. **B333**, 420 (1994); hep-ph-9406204.
S. Hashimoto, J. Kodaira and Y. Yasui, hep-ph-9406271.